

# DYNAMICS AND THERMODYNAMICS OF PHASE TRANSITION IN HOT NUCLEI

M. F. Rivet,<sup>1,\*</sup> N. Bellaize,<sup>2</sup> B. Borderie,<sup>1</sup> R. Bougault,<sup>2</sup> A. Chbihi,<sup>3</sup> J.D. Frankland,<sup>3</sup> B. Guiot,<sup>3</sup> O. Lopez,<sup>2</sup> N. Le Neindre,<sup>2</sup> M. Pârlog,<sup>4</sup> G. Tăbăcaru,<sup>4</sup> J.P. Wieleczko,<sup>3</sup> G. Auger,<sup>3</sup> Ch.O. Bacri,<sup>1</sup> B. Bouriquet,<sup>3</sup> A.M. Buta,<sup>2</sup> J. Colin,<sup>2</sup> D. Cussol,<sup>2</sup> R. Dayras,<sup>5</sup> N. de Cesare,<sup>6</sup> A. Demeyer,<sup>7</sup> D. Doré,<sup>5</sup> D. Durand,<sup>2</sup> E. Galichet,<sup>1,8</sup> E. Gerlic,<sup>7</sup> D. Guinet,<sup>7</sup> S. Hudan,<sup>3</sup> G. Lanzalone,<sup>1,†</sup> P. Lantesse,<sup>7</sup> F. Lavaud,<sup>1</sup> J.L. Laville,<sup>3</sup> J.F. Lecomte,<sup>2</sup> R. Legrain,<sup>5,‡</sup> L. Nalpas,<sup>5</sup> J. Normand,<sup>2</sup> P. Pawłowski,<sup>1</sup> E. Plagnol,<sup>1</sup> E. Rosato,<sup>6</sup> R. Roy,<sup>9</sup> J.C. Steckmeyer,<sup>2</sup> B. Tamain,<sup>2</sup> E. Vient,<sup>2</sup> M. Vigilante,<sup>6</sup> and C. Volant<sup>5</sup>

(INDRA collaboration)

<sup>1</sup>Institut de Physique Nucléaire, IN2P3-CNRS, F-91406 Orsay Cedex, France.

<sup>2</sup>LPC, IN2P3-CNRS, ISMRA et Université, F-14050 Caen Cedex, France.

<sup>3</sup>GANIL, CEA et IN2P3-CNRS, B.P. 5027, F-14076 Caen Cedex, France.

<sup>4</sup>Nat. Inst. for Physics and Nuclear Engineering, Bucharest-Măgurele, Romania.

<sup>5</sup>DAPNIA/SPhN, CEA/Saclay, F-91191 Gif sur Yvette, France.

<sup>6</sup>Dip. di Scienze Fisiche e Sez. INFN, Univ. di Napoli “Federico II”, Napoli, Italy.

<sup>7</sup>Institut de Physique Nucléaire, IN2P3-CNRS et Université F-69622 Villeurbanne, France.

<sup>8</sup>Conservatoire National des Arts et Métiers, F-75141 Paris Cedex 03.

<sup>9</sup>Laboratoire de Physique Nucléaire, Université Laval, Québec, Canada.

## Abstract

The dynamics and thermodynamics of phase transition in hot nuclei are studied through experimental results on multifragmentation of heavy systems ( $A \geq 200$ ) formed in central heavy ion collisions. Different signals indicative of a phase transition studied in the INDRA collaboration are presented and their consistency is stressed.

## 1. INTRODUCTION

Liquid-gas type phase transitions are commonly observed in systems with short-range repulsive and longer-range attractive forces, such as macroscopic fluids with the van der Waals interaction. The nuclear equation of state is very similar to that of non-ideal gases, which allows to foresee the existence of different phases of nuclear matter. But can one define phase transitions in “small” objects, when the dimension is of the same order of magnitude as the range of the force which binds them? In this sense nuclei as well as clusters of galaxies are small. Recent works state that statistical mechanics based on the Boltzmann’ definition of entropy ( $S =$

$k \cdot \log W$ ) allows to define phase transitions in small systems [1]. The nucleus at zero or moderate temperature, because of its quantal nature, is assimilated to a liquid phase. A nuclear gas phase was characterized, for instance, through the properties of vaporised quasi-projectiles from 95 A MeV Ar+Ni reactions, fully predicted by modelling a van der Waals gas of fermions and bosons in thermodynamic equilibrium [2]. The liquid-gas coexistence region was thus naturally connected to multifragmentation, break-up of a nuclear system in several fragments of various sizes.

Most of the works on nucleus phase transition relied on static properties such as the charge (or mass) partitions measured in nuclear reactions. The observation of a power law on a limited range of fragment charge measured in inclusive experiments was claimed to be consistent with a critical behaviour, according to Fisher’s droplet

\*e-mail:rivet@ipno.in2p3.fr

†Permanent address: Laboratorio Nazionale del Sud, Via S. Sofia 44, I-95123 Catania, Italy.

‡deceased

model [3], and also to percolation models [4]. Recent and well selected data from the ISIS collaboration were analysed in this framework, and a liquid-gas coexistence curve was derived [5, 6]. In the same line, critical exponents were reported to have measured values in agreement with those of a liquid-gas model [7, 8].

Caloric curves relate the energy and the temperature of nuclei. The observation of caloric curves showing a bending or a plateau, similar to what is observed for the boiling of water, was claimed as a proof of the nuclear phase transition [9].

A new signal of phase transition of nuclei was found in the observation of a negative branch of the microcanonical heat capacity for Au quasi-projectiles excited between 3 and 6 AMeV [10].

This paper presents a compilation of the results which deal with *central collisions* between heavy ions ( $A_{proj} + A_{tgt} > 200$ ), obtained so far in the INDRA collaboration. Most of them will be detailed in other contributions to this conference. Different signals which may be connected with the occurrence of a phase transition in nuclei were found, each of them bringing a small stone to the construction of a consistent framework.

## 2. PHASE TRANSITION: DYNAMICS AND THERMODYNAMICS

### 2.1. Thermodynamics aspect

As exemplified in fig. 1, where isotherms are drawn in a pressure-density plane, the EOS of nuclear matter resembles that of a van der Waals gas. A region of negative incompressibility, bordered by the spinodal line, and located inside the coexistence region, appears in this diagram. This spinodal region is a zone of mechanical instability, where an increase of pressure leads to an expansion of the system; on entering this zone the system will tend to recover thermodynamical equilibrium by separating into two coexisting phases, a low-density (gas) phase and a higher density (liquid) phase. Note that the time for the system to go from homogeneity to inhomogeneity is finite, in other words a phase transition has a dynamics (see next subsection). The spinodal region is also thermally unstable, as the heat capacity,  $c = dE/dT$ , is negative inside this zone. Ac-

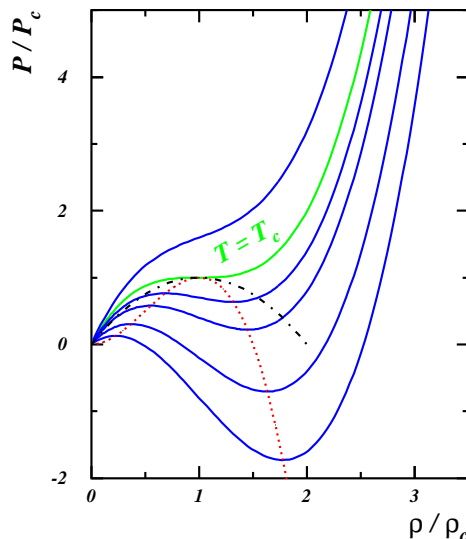


Fig. 1: Equation of state relating the pressure and the density (normalised to the critical values) in nuclear matter. The curves represent isotherms. The dashed-dotted line is the coexistence line and the dotted line the spinodal line.

ording to this formula, it seems easy to evidence a negative heat capacity, which should appear, in a microcanonical frame, as a backbending of the caloric curve. It is not so simple in the case of nuclei, as their temperature, energy, density can only be modified by a more or less violent nuclear collision; one is dealing with isolated systems without external constraints, which eventually induce a phase transition in the course of their evolution in a (temperature, pressure, energy) space. The followed path is not known and there is no *a priori* reason why the resulting caloric curve would have a plateau, or a backbending [11]. Another and more robust signal was proposed to recognise a phase transition, abnormally large fluctuations of the kinetic part,  $E_k$  of the energy ( $E = E_k + E_{pot}$ ) [12]. In this case the heat capacity can be expressed as  $c_{tot} = c_k^2 / (c_k - A\sigma_k^2/T^2)$ , with  $c_k = d\langle E_k \rangle / dT$ . When the normalised fluctuations exceed the canonical value  $c_k$ , the heat capacity becomes negative, as depicted in fig. 2. These variables may be determined in an experiment, provided that one can reconstruct the partition present at the “freeze-out” stage, defined as the instant when nuclear interaction between the present species vanishes.

Finally this static statistical physics approach supposes that the ensemble of collisions considered constitutes a statistical ensemble. This en-

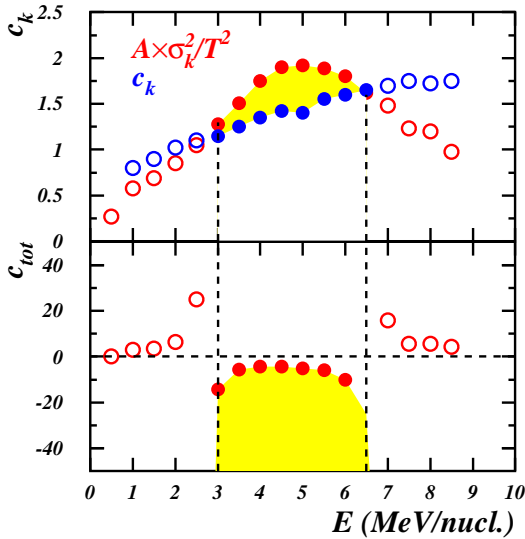


Fig. 2: Variation versus energy of the kinetic fluctuations and heat capacity (top) and of the total heat capacity (bottom).

semble is characterized by global variables reflecting the pertinent information resulting from the dynamics of the collisions or (and) the sorting of the events. Statistical physics concepts can be safely used providing that there is adequacy between the ensemble treated and the applied formalism [13].

## 2.2. Dynamics of the phase transition

Is it possible to explore the fugitive dynamics of the nuclear phase transition? A positive answer was recently given in the INDRA collaboration. Heavy nuclear systems were produced at the same energy ( $\sim 7$  AMeV), but with very different total masses (393 and 248), through central collisions between 36 AMeV Gd and U and 32 AMeV Xe and Sn; the resulting measured charge distributions superimposed while the fragment multiplicities scaled as the total system masses [14]. While this indicates the dominance of phase space effects, with stochastic fragment production governed by a Boltzmann factor, it may also sign the presence of bulk instabilities inducing density fluctuations, and finally leading to the spinodal decomposition of the nuclear system. And indeed spinodal decomposition is, together with nucleation, one of the processes describing the dynamics of the liquid-gas phase transition in nuclear matter [15]. The most

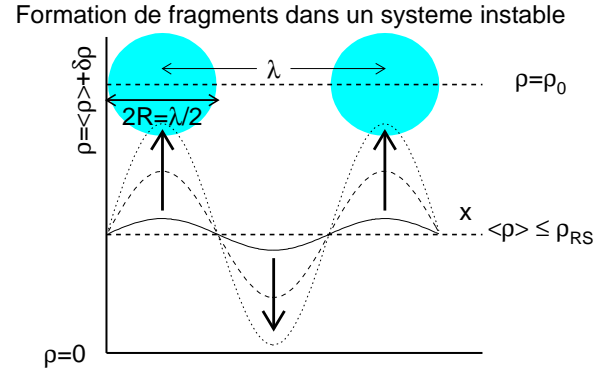


Fig. 3: Density fluctuations and fragment formation in the spinodal region [16].

unstable mode(s) in the system induce homogeneous density fluctuations which will be amplified by the mean field with a characteristic time which decreases with the temperature of the system. Locally zones close to normal density may appear, leading to the formation of fragments whose radii and relative distances depend on the wavelength of the mode, as schematized in fig. 3. In this scenario, one expects a narrow fragment charge distribution, loosely dependent on the total charge of the system provided it is large enough. In finite size hot nuclear systems several modes are equally probable, may beat, all effects which blur the initial picture and lead to much broader charge distributions. This is ex-

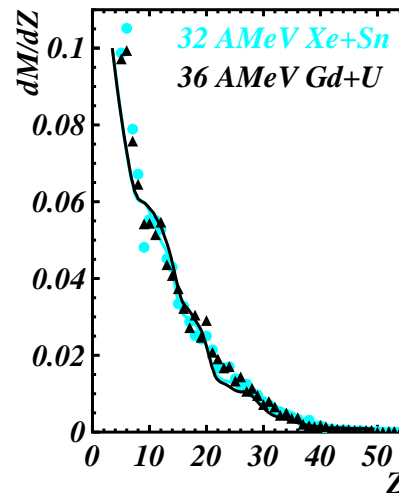


Fig. 4: Charge distributions from central heavy ion collisions. The lines show the results of stochastic mean field simulations while the symbols display the experimental results. Adapted from [17].

emplified in fig. 4, where the lines display the

charge distributions obtained through a complete stochastic mean field simulation of central nuclear collisions between heavy ions, the Brownian one-body dynamics (Bob): the mean field is complemented by a Brownian force in the kinetic equations, which mimic a stochastic collision term. For the two reactions considered here, 36 AMeV Gd+ U, and 32 AMeV Xe+Sn, the system is driven into the spinodal region, where it multifragments through spinodal decomposition [18]. The de-excitation of the hot fragments so formed is followed simultaneously with their propagation in their Coulomb field. Finally the simulated events (Bob events) are passed through a software replica of the INDRA detector. Obviously the final distributions (lines in fig. 4) are far from narrow, being continuously decreasing with increasing  $Z$  without any visible peak. But they perfectly reproduce the experimental distributions measured in the two systems quoted above (symbols in fig. 4), particularly the independence of the charge distribution against the mass of the system is recovered [17]. It is worthwhile to mention that kinetic properties of the outgoing channel are also well accounted for, particularly the fragment-fragment velocity correlations [19].

These simulations show that the phase transition, or the spinodal decomposition process can not be evidenced by a single variable like a charge distribution. It might however well be that a few events kept a memory of the process, through a preferred break-up in equal-sized fragments. The charge correlation function defined as:  $C = Y_{cor}(Z_{av}, \sigma_Z)/Y_{uncor}(Z_{av}, \sigma_Z)$  is very efficient to enlighten any extra production of rare event types [20], as it makes use of the full per-event information through two variables, the average charge  $Z_{av}$  and the standard deviation  $\sigma_Z$ . Equal-sized fragment partitions (small  $\sigma_Z$ ), were looked for in Bob events from 32 AMeV Xe+Sn central collisions. The variable  $Z_{av}$  was replaced by  $M_f \times Z_{av}$  as events with different fragment multiplicities  $M_f$  were mixed to improve statistics [21]. The uncorrelated yield,  $Y_{uncor}(Z_{av}, \sigma_Z)$ , obtained in ref [20, 21] by making pseudo-events from fragments belonging to different events of the same sample, may also be analytically calculated from the charge dis-

tribution [22], in order to make its statistical error negligible everywhere. The correlation function shown in fig. 5 (left) uses the analytical  $Y_{uncor}$  and the standard deviation of the measure:  $\sigma_Z = (\sum_{i=1}^{M_f} (Z_i - Z_{av})^2 / M_f)^{1/2}$ , at variance with ref [20, 21], The general trend is a decrease of the correlation function with decreasing  $\sigma_Z$ , as expected from the broad charge distribution, except in the smaller bin,  $\sigma_Z < 1$ , where it increases again. For  $36 < M_f \times Z_{av} < 60$  this increase is statistically significant, with a confidence level larger than 98%. But only 0.6% of the events contribute to these enhanced partitions, while all simulated events multifragment through spinodal decomposition. Due to this small number one may wonder about the real meaning of these peaks at small  $\sigma_Z$ , because their statistical significance must be weighted against a “background”, corresponding to the extrapolation of the trend of the measured correlation function for decreasing  $\sigma_Z$ . This extrapolation was empirically performed with an exponential function [21]. The method was recently improved by building the uncorrelated yield following an independent emission model under the constraint of charge conservation of the *total system* [22]. The result, on the same Bob event sample, is shown in the right part of fig. 5. All correlations due to charge conservation are now suppressed, and the correlation function is equal to 1 wherever no additional physical correlation is present. To make the picture stronger, the peaks with a significance lower than 95% have been flattened out in fig. 5 (right). Again one observes peaks for small values of  $\sigma_Z$ , the percentage of events concerned is 0.7%, which fully validates the published results [21].

In short simulations of central heavy ion collisions show that fingerprints of the spinodal decomposition of a nuclear system can be found, namely a weakly but unambiguously enhanced proportion of equal-sized fragment partitions, and thus evidence its phase transition. A statistical model, like any model just based on phase space, will not show this type of phenomenon [22].

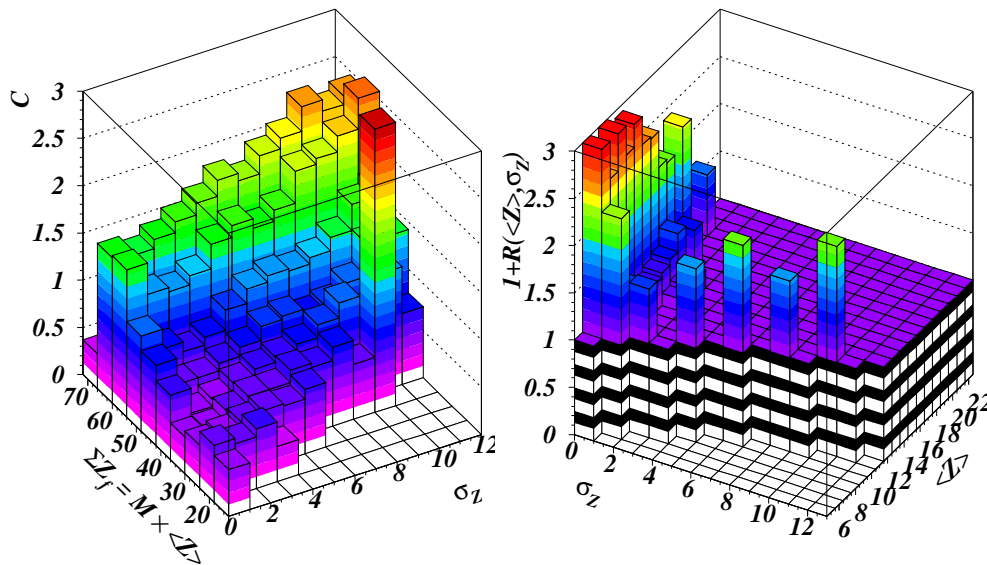


Fig. 5: Charge correlation function for events generated by stochastic mean field simulations of central 32 AMeV Xe+Sn collisions, without (left) and with (right) charge conservation constraint on the uncorrelated yields. Note the different orientation of the two figures. The charge axes are  $M_f \times Z_{av}$  on the left, and  $Z_{av}$  on the right, while the  $\sigma_Z$  axes are the same. In both cases events with 3 to 6 fragments are included.

### 3. EXPERIMENTAL INDICATIONS OF MULTIFRAGMENTATION IN THE SPINODAL REGION

Two reactions were studied by the INDRA collaboration which lead to systems with close total mass and charge ( $Z \sim 105$ ,  $A \sim 250$ ). The symmetric Xe+Sn system was studied between 25 and 50 AMeV, and a class of events characterized as multifragmentation of “fused” systems was recognized at and above 32 AMeV. Event selection was performed on completeness and event shape criteria, and the multifragmentation of deformed objects was not considered in these samples [17, 23]. The asymmetric Ni+Au system was studied from 32 to 90 AMeV. Owing to the thresholds of INDRA, and to the smaller c.m. velocity for this asymmetric entrance channel, the number of complete events is very small. Methods selecting classes of events were developed, less stringent on completeness requirements. Two of these methods were used for isolating events samples of central collisions with close distributions of global observables: the Principal Component Analysis method [24, 25]) for the sample on which the heat capacity was determined and the Discriminant Factorial Analysis method [26]) for the sample used for charge correlations.

#### 3.1. The symmetric entrance channel

The heat capacity and the charge correlations were both examined in the same samples of Xe+Sn central collisions. Charge correlations are presented in fig. 6, for the four incident energies [27]. The correlation functions shown here are calculated without the charge conservation constraint, and the figure only presents them for the first bin  $\sigma_Z \in [0 - 1]$ . The data corresponding to an enhanced production of equal-sized fragment partitions with a high confidence level are indicated by darker points. This enhancement is only observed at 32 and 39 AMeV, and correspond to 0.2 and 0.4% of the selected samples. These percentages are close to those observed in the Bob simulations, and may be interpreted in stating that the dynamics of multifragmentation occurs by spinodal decomposition in all the selected central collisions.

The heat capacity was determined on reconstructed freeze-out configurations out of the measured data [28]. The excitation energy scale was obtained by calorimetry, including all measured fragments and twice the light charged particles emitted between 60 and 120deg in the c.m. Neutrons were estimated from mass conservation. The radial expansion energy was deter-

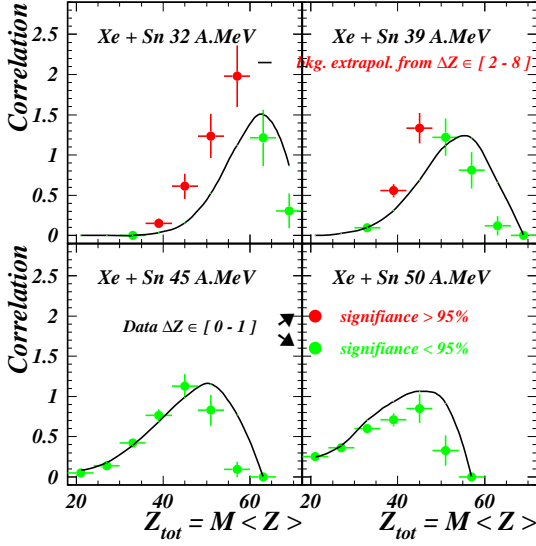


Fig. 6: Charge correlation functions (without charge conservation constraint) for central collision events between Xe and Sn. The lines indicate the extrapolated background. The darker points correspond to event partitions enhanced with a high significance. From [27]

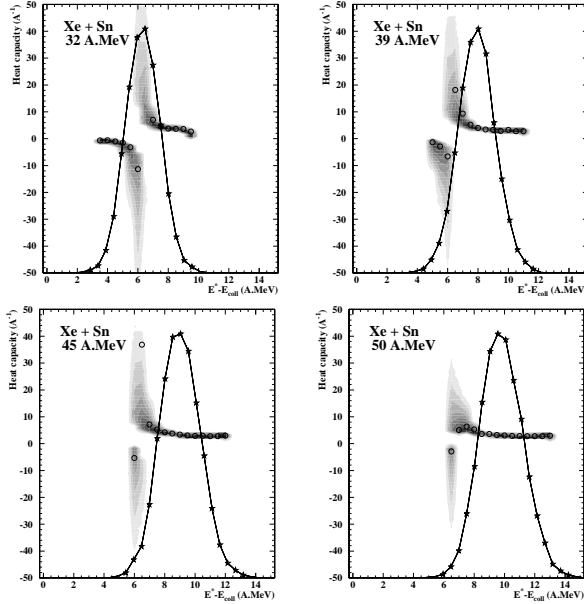


Fig. 7: Heat capacity versus the excitation energy (corrected for the collective energy) measured in central collisions between Xe and Sn. From [28]

mined from a comparison of the data with results of a statistical multifragmentation model, and was subtracted from the excitation energy to give the energy distributions shown by the lines in fig. 7. The potential energy was taken as the sum of the mass balance and of the Coulomb energy estimated through the Wigner-Seitz approximation, with a freeze-out volume  $V = 3 \times V_0$ .

The influence of these assumptions on the amplitude of the fluctuations is thoroughly discussed in [29]. The heat capacity, derived as explained in sect. 2.2.1, is plotted as grey zones (error bars) in fig. 7. Negative branches are observed below  $E^* = 6-6.5$  A.MeV at the four incident energies. At 32 and 39 A.MeV there is a significant overlap between the energy distribution and the negative heat capacity; this indicates that multifragmentation occurred in the spinodal region, in agreement with the signal given by the charge correlations. At and above 45 A.MeV, both the non observation of enhanced equal-size fragment partitions and the positive value of the heat capacity plead for the system multifragmenting in the coexistence region outside the spinodal zone.

### 3.2. The asymmetric entrance channel

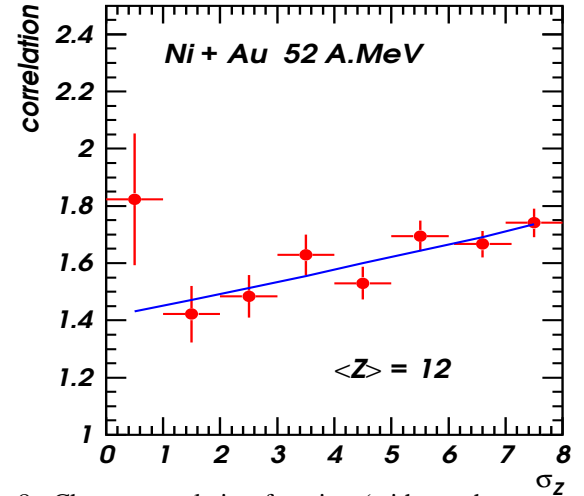


Fig. 8: Charge correlation function (without charge conservation constraint) versus the standard deviation  $\sigma_Z$  for a given value  $Z_{av} = 12$ . The line indicates the linear background. From [30]

Enhanced partitions of equal-sized fragments were looked for in central Ni+Au collisions at 32 and 52 A.MeV [31]. A statistically significant enhancement only appeared at 52 A.MeV, as shown in fig. 3.3.2, where the correlation function is calculated without charge conservation constraint. Results with the new method can be found in the contribution of B. Guiot, and agree with the above statement.

The heat capacity was calculated for incident energies of 32, 52, 74 and 90 A.MeV. Precisions on the implied assumptions are detailed in the

contribution of O. Lopez to this conference, in which the results are also unveiled. The energy scale is here obtained from calorimetry, using products emitted between 60 and 120deg *c.m.* whatever their charge, due to stronger contributions of forward preequilibrium emissions with respect to the symmetric entrance channel. A negative branch of the heat capacity appears below 6-7 AMeV at the four incident energies. The data at 32 AMeV should be taken with caution, as the average completeness of the events is poor (65% of the total charge). Indeed because of the low value of the average excitation energy (3.5 AMeV), one would expect to observe the first divergence of the heat capacity, while only the second one is seen, in the higher part of the energy distribution. At the three other incident energies, the average excitation energy varies little (5.5, 7, 7 AMeV) and the heat capacity is negative in the first half of the distribution.

For this asymmetric entrance channel, multifragmentation in the spinodal region is shown by dynamical and thermodynamical signals at 52 AMeV only. For collisions at higher energy only the negative heat capacity was looked for, and found. At 32 AMeV there is no sign of spinodal decomposition, and the data resemble more a fusion-evaporation process [24]; surprisingly only the negative part of the heat capacity was observed despite the low excitation energies covered.

#### 4. NEW SIGNALS EVIDENCING A PHASE TRANSITION

##### 4.1. Universal fluctuations of an order parameter

The recently developed theory of universal fluctuations in finite systems provides methods to characterize critical and off-critical behaviours, without any equilibrium assumption [33]. In this framework, universal  $\Delta$  scaling laws of one of the order parameters,  $p$ , should be observed:

$$\langle p \rangle^\Delta P(p) = \phi((p - p^{mp})/\langle p \rangle^\Delta)$$

where  $p^{mp}$  stands for the most probable value of  $p$ .  $\Delta=1/2$  corresponds to small fluctuations,  $\sigma_p^2 \sim \langle p \rangle$ , and thus to an ordered phase. Conversely  $\Delta=1$  occurs for the largest fluctuations nature provides,  $\sigma_p^2 \sim \langle p \rangle^2$ , in a disordered phase.

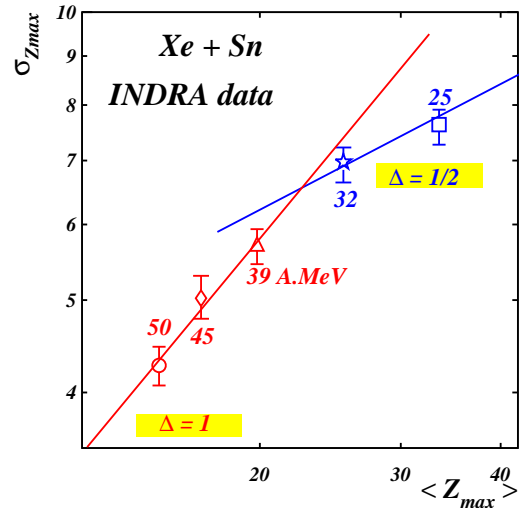


Fig. 9: Normalised first and second moments of the scaled distributions of the event heaviest fragments, for Xe+Sn central collisions at five incident energies. The lines  $\Delta = 1$  and  $1/2$  are shown to guide the eye. Note the two logarithmic scales. Adapted from [32].

Scaling laws may be expected for an order parameter  $p$  increasing with time, for instance the fragment multiplicity in a fragmentation process, or the largest fragment size in an aggregation process. The method was applied to the Xe+Sn central collision samples described in sect. 3, extended to the measurements performed at 25 AMeV [32]. The fragment multiplicity distributions at the five energies scale with a small variance ( $\Delta=1/2$ ), while the largest fragment distributions follow a  $\Delta=1/2$  scaling at low energy (25 and 32 AMeV) and a  $\Delta=1$  scaling for the three highest energies; fig. 9 illustrates the variation of  $\sigma_{Zmax}$  vs.  $Z_{max}$ . Following the authors of this study, this indicates the transition from an ordered phase (evaporation?) to a disordered phase, the fragments being produced following an aggregation scenario. Note that spinodal decomposition well enters this type of scenario.

##### 4.2. Bimodality of an order parameter

An extended definition of first order phase transitions in finite systems was proposed in [34], based on topology anomalies of the event distribution in the space of observation. In this framework when a nuclear system is in the coexistence region, the probability distribution of an order parameter is bimodal, each component being a phase. The Xe+Sn central collisions samples

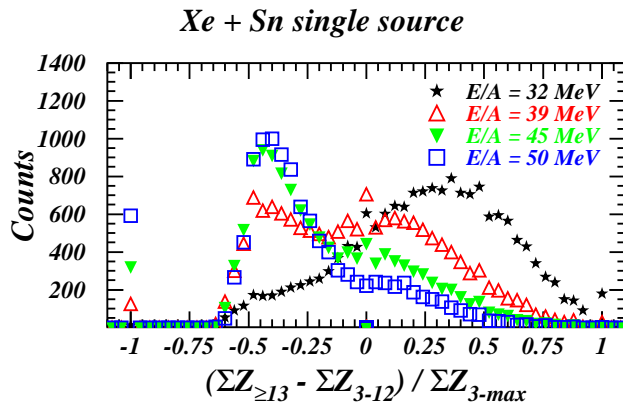


Fig. 10: Distributions of the differences of total charges bound in big ( $Z \geq 13$ ) and small ( $Z \in [3 - 12]$ ) fragments in events from Xe+Sn central collisions. From [27]

were also analysed this way. Having in mind the liquid-gas coexistence region, one has to guess which fragments belong to each of the phases. Owing to the detailed shape of the charge distributions [27],  $Z=12$  was tentatively put as a limit between the two phases. The chosen sorting parameter,  $(\sum Z_{Z \geq 13} - \sum Z_{Z \in [3-12]}) / \sum Z_{Z \geq 3}$ , may be connected with the density difference of the two phases ( $\rho_L - \rho_G$ ), which is an order parameter [13]. The results are displayed in fig. 10: none of the distribution is Gaussian, which would sign a pure phase; but the gas phase is dominant above 45 AMeV, while the liquid phase is more important at 32 AMeV. The two components are roughly equal at 39 AMeV.

Similar results were obtained on the Ni+Au central collision samples selected with the PCA. A similar sorting parameter, making use of only the three largest fragments, was used. Its probability distribution exhibits two nearly equal peaks at 32 AMeV, a big “gas” peak with a small shoulder at 52 AMeV and a single phase picture at 90 AMeV [25].

## 5. SYNTHESIS OF THE OBSERVATIONS FOR SYSTEMS OF 250 NUCLEONS

A synthesis of the signals which may sign a liquid-gas phase transition for nuclei of mass  $\sim 250$  is presented in table I. The thermal and radial energy scales come from SMM simulations, with respective uncertainties of 1 and 0.5 AMeV,

depending, for instance, on the event selections, the freeze-out volume chosen ... [24, 28]. The first evidence coming from this table is that for the asymmetric entrance channel, multifragmentation of the fused system formed in central collision is *not* associated to a radial expansion. This comes at variance of other results for similar systems in the same energy range, for instance Kr+Au [35]. Note that the result comes directly out of the data, as for Xe+Sn at 50 AMeV and Ni+Au at 90 AMeV, the partitions are similar, while the average kinetic energies of a given fragment strongly differ, and are constant for  $Z$  between 12 and 30 for the latter system [25]

For both entrance channels, the systems reach the spinodal region and remain there for a time sufficient to allow the development of spinodal instabilities for thermal energies between 5 and 6.5 AMeV, as attested by the observation of favoured equal-sized fragment partitions and the negative values of the heat capacities. When the thermal energy increases, the expansion energy seems to have a decisive role: without expansion, the picture is similar to the one just described, up to  $\varepsilon_{th} = 7.5$  AMeV, while an expansion energy above 25% of the thermal energy would make the system cross too fast the spinodal region, toward the coexistence region or even the gas region. In this case neither the spinodal decomposition nor the negative heat capacity are observed. The critical excitation energy, given by the maximum thermal energy of the systems described in this paper and shown to have fragmented in the spinodal region is at least 7.5 AMeV, much above the value given in [5]. It must however be noted that the “multifragmentation” partitions analysed in this reference comprise essentially one large cluster and one intermediate mass fragment, together with nucleons and light charged particles [36], at variance with the partitions observed in the INDRA data which have a larger number of fragments. In this sense the “critical” values of [5] would rather be assimilated to “limiting” temperatures, or excitation energies, as described in [37]. Above limiting values, a nucleus is unstable due to Coulomb forces, and can only de-excite through multifragmentation.

What additional information is brought by the other signals quoted in table I? The universal



Table I: Summary of the phase transition signals described in the previous sections.  $\varepsilon_{inc}$ ,  $\varepsilon_{th}$ ,  $\varepsilon_{rad}$ , stand for the incident, thermal and expansion energies in AMeV (see text for precisions). SD means signal of spinodal decomposition.  $\Delta$  indicates the exponent of the universal scaling, and the Bimod line gives the number of peaks in the probability distribution ( $\textcircled{2}$  means two equal peaks). A “-” means that no measurement of the concerned observable was done.

| system              | Ni+Au             | Xe+Sn | Xe+Sn             | Ni+Au  | Xe+Sn | Xe+Sn | Ni+Au | Ni+Au      |
|---------------------|-------------------|-------|-------------------|--------|-------|-------|-------|------------|
| $\varepsilon_{inc}$ | 32.               | 32.   | 39.               | 52.    | 45.   | 50.   | 74.   | 90.        |
| $\varepsilon_{th}$  | 5.0               | 5.0   | 6.0               | 6.5    | 6.6   | 7.0   | 7.0   | 7.5        |
| $\varepsilon_{rad}$ | 0.                | 0.6   | 1.2               | 0.     | 1.7   | 2.0   | 0.    | $\leq 0.5$ |
| SD                  | no                | yes   | yes               | yes    | no    | no    | -     | -          |
| $c < 0$             | yes               | yes   | yes               | yes    | no    | no    | yes   | yes        |
| $\Delta$            | -                 | 1/2   | 1                 | -      | 1     | 1     | -     | -          |
| Bimod.              | $\textcircled{2}$ | 2     | $\textcircled{2}$ | 1 or 2 | 2     | 2     | -     | 1          |

fluctuations are small for  $\varepsilon_{th} \leq 5$  AMeV, and large above ( $\Delta = 1$ ). This can be interpreted as the transition from the dominance of fusion evaporation to that of fusion-multifragmentation processes around this energy; indeed at 32 AMeV the selected central collisions in Ni+Au present essentially the characteristics of an evaporation process [24]. In this sense, large fluctuations of  $Z_{max}$  would sign the break-up of the system inside the coexistence region. Bimodality of a parameter related to the density of the system goes roughly in the same direction. Two peaks, indicating that the systems break in the coexistence region, are observed in all the cases except for Ni+Au at 90 AMeV. This would indicate a pure gas phase, and contradict somewhat the measurement of a negative heat capacity. The equal abundance of the two phases occurs for  $\varepsilon_{th} \leq 5-6$  AMeV, above that energy nuclear systems would mainly multifragment.

## 6. CONCLUSIONS AND PERSPECTIVES

The results obtained in analysing central collisions leading to  $A \sim 250$  systems through a symmetric and an asymmetric entrance channel show several features which may be taken as characteristics of a liquid-gas phase transition in nuclei. While each of these signals may not be conclusive by itself, their concomitance gives strength to the assumed scenario. In the next future, one may try to find other variables or signals which would support the existence of the phase transition. It is also worth looking to all these signals for quasi-projectile nuclei, of which INDRA possess a tremendous collection, spanning Ar, Ni,

Xe, Gd, Ta, U projectiles.

Next, enriched knowledge of nuclear matter properties will come from taking into account its two component nature (neutrons and protons), by exploring collisions induced by exotic projectiles when they are available. Isospin fractionation should allow to distinguish the liquid and gas phases.

## Acknowledgments

All the exciting results presented in this paper were understood through their sharing with theoreticians. The INDRA collaboration is indebted to P. Chomaz, M. Colonna, P. D esesquelles, F. Gulminelli and M. Płoszajczak for their essential contribution through many discussions.

## 7. REFERENCES

- [1] D. H. E. Gross, cond-mat/0105313.
- [2] B. Borderie and INDRA collaboration, Eur. Phys. J. 6 (1999) 197.
- [3] M. E. Fisher, Physics 3 (1967) 255.
- [4] J. B. Elliott et al., Phys. Rev. Lett. 85 (2000) 1194.
- [5] J. B. Elliott et al., nucl-ex/0104013.
- [6] L. G. Moretto, in Proc. Int. Workshop on Multifragmentation 2001, Catania, Italy, 2001 .
- [7] J. B. Elliott and EOS collaboration, Phys. Lett. B 418 (1998) 34.
- [8] M. D’Agostino et al., Nucl. Phys. A 650 (1999) 329.
- [9] J. Pochodzalla and ALADIN collaboration, Phys. Rev. Lett. 75 (1995) 1040.
- [10] M. D’Agostino et al., Phys. Lett. B 473 (2000) 219.

- [11] P. Chomaz, V. Duflot and F. Gulminelli, *Phys. Rev. Lett.* 85 (2000) 3587.
- [12] P. Chomaz and F. Gulminelli, *Nucl. Phys. A* 647 (1999) 153.
- [13] F. Gulminelli, in *Proc. Int. Workshop on Multifragmentation 2001*, Catania, Italy, 2001 .
- [14] M. F. Rivet and INDRA collaboration, *Phys. Lett. B* 430 (1998) 217.
- [15] D. Idier, M. Farine, B. Remaud and F. Sébille, *Ann. Phys. Fr.* 19 (1994) 159.
- [16] J. D. Frankland, Ph.D. thesis, Université Paris XI Orsay, (1998), IPNO-T-98-06.
- [17] J. D. Frankland and INDRA collaboration, *Nucl. Phys. A* 689 (2001) 940.
- [18] A. Guarnera et al., *Phys. Lett. B* 373 (1996) 267.
- [19] G. Tăbăcaru and INDRA collaboration, in *Nucleus-Nucleus collisions*, Proc. of the International Conference on Structure of the Nucleus at the Dawn of the Century, Bologna, Italy, edited by G. Bonsignori, M. Bruno, A. Ventura and D. Vretenar, World Scientific, 2000 p. 321.
- [20] L. G. Moretto et al., *Phys. Rev. Lett.* 77 (1996) 2634.
- [21] B. Borderie and INDRA collaboration, *Phys. Rev. Lett.* 86 (2001) 3252.
- [22] P. Désesquelles, *Phys. Rev. C* (2001), In press and nucl-ex/0109019.
- [23] B. Bouriquet, Ph.D. thesis, Université de Caen, (2001), GANIL T 01 02.
- [24] N. Bellaize and INDRA collaboration, in *Proc. XXXIX Int. Winter Meeting on Nuclear Physics*, Bormio, Italy, edited by I. Iori, *Ricerca scientifica ed educazione permanente*, 2001 p. 183.
- [25] O. Lopez and INDRA collaboration, in *Proc. XXXIX Int. Winter Meeting on Nuclear Physics*, Bormio, Italy, edited by I. Iori, *Ricerca scientifica ed educazione permanente*, 2001 p. 61.
- [26] P. Désesquelles and INDRA collaboration, *Phys. Rev. C* 62 (2000) 024614.
- [27] B. Borderie and INDRA collaboration, in *Proc. XXXIX Int. Winter Meeting on Nuclear Physics*, Bormio, Italy, edited by I. Iori, *Ricerca scientifica ed educazione permanente*, 2001 p. 73, nucl-ex/0106007.
- [28] R. Bougault and INDRA collaboration, in *Proc. XXXVIII Int. Winter Meeting on Nuclear Physics*, Bormio, Italy, edited by I. Iori, *Ricerca scientifica ed educazione permanente*, 2000 p. 404.
- [29] M. D'Agostino et al., *Nucl. Phys. A* (2002), In press, and nucl-ex/0104024.
- [30] B. Guiot and INDRA collaboration, to be published.
- [31] B. Guiot and INDRA collaboration, in *Proc. Int. Workshop on Multifragmentation 2001*, Catania, Italy, 2001 .
- [32] R. Botet et al., *Phys. Rev. Lett.* 86 (2001) 3514.
- [33] R. Botet and M. Płoszajczak, *Phys. Rev. E* 62 (2000) 1825.
- [34] P. Chomaz, F. Gulminelli and V. Duflot, *Phys. Rev. E* 64 (2001) 046114.
- [35] C. Williams et al., *Phys. Rev. C* 55 (1997) 2132.
- [36] L. Beaulieu et al., *Phys. Rev. C* 63 (2001) 031302R.
- [37] S. Levit and P. Bonche, *Nucl. Phys. A* 437 (1985) 426.